

## HYDRODYNAMIC EXPERIMENTS ON A SMALL-SCALE CIRCULATING FLUIDIZED BED REACTOR AT ELEVATED OPERATING PRESSURE, AND UNDER AN O<sub>2</sub>/CO<sub>2</sub> ENVIRONMENT

by

**Yerbol SARBASSOV<sup>a</sup>, Azd ZAYOUD<sup>b</sup>, Pinakeswar MAHANTA<sup>b</sup>, Sai GU<sup>a</sup>,  
Panneerselvam RANGANATHAN<sup>a</sup>, and Ujjwal K. SAHA<sup>b</sup>**

<sup>a</sup> School of Energy, Environment and Agrifood, Cranfield University, Cranfield, UK

<sup>b</sup> Mechanical Engineering Department, Indian Institute of Technology Guwahati,  
Guwahati, Assam, India

Original scientific paper

<https://doi.org/10.2298/TSCI150921068S>

*Pressurized circulating fluidized bed technology is a potentially promising development for clean coal technologies. The current work explores the hydrodynamics of a small-scale circulating fluidized bed at elevated operating pressures ranging from 0.10 to 0.25 MPa. The initial experiments were performed at atmospheric pressure with air and O<sub>2</sub>/CO<sub>2</sub> environments as the fluidization gas to simulate the hydrodynamics in a circulating fluidized bed. A comparison between the effects of air and O<sub>2</sub>/CO<sub>2</sub> mixtures on the hydrodynamics was outlined in this paper for particles of 160 μm diameter. A small but distinct effect on axial voidage was observed due to the change in gas density in the dense zone of the bed at lower gas velocity, while only minimal differences were noticed at higher gas velocities. The hydrodynamic parameters such as pressure drop and axial voidage profile along the height were reported at two different bed inventories (0.5 and 0.75 kg) for three mean particle sizes of 160, 302, and 427 μm and three superficial gas velocities. It was observed that the operating pressure had a significant effect on the hydrodynamic parameters of bed pressure drop and axial bed voidage profiles. The effect of solids loading resulted in an exponential change in pressure drop profile at atmospheric pressure as well as at elevated pressure. The experimental results on hydrodynamic parameters are in reasonable agreement with published observations in the literature.*

Key words: *circulating fluidized bed, pressurized circulating fluidized bed, pressure drop, axial voidage profile, O<sub>2</sub>/CO<sub>2</sub> mixture*

### Introduction

Currently, 40% of the world's electricity is generated by coal-fired power plants which consequently are a major contributor to climate change due to GHG emissions, mainly CO<sub>2</sub> [1]. Further research on development of clean coal technology and carbon capture and storage technology is required to reduce emissions from heavy industry and power plants. Circulating fluidized bed (CFB) technologies, have been developed commercially over the past 50 years, and are utilized in clean coal technologies to produce electricity [2]. However, the technology is still evolving and it is possible to increase the energy efficiency of the CFB power plants. The CFB technology has a number of advantages over pulverized

\* Corresponding author, e-mail: y.sarbassov@cranfield.ac.uk

coal boilers such as the ability to utilize low-rank coals, and provide a wider turndown capacity [3-5]. Nowak [5] have outlined the advantages of CFB technologies built in Poland between 1996 and 2003. Recently, CanmetENERGY [6, 7] has developed various oxy-fuel CFB reactors with capacity range of 0.1 to 0.8 MW. Moreover, Foster Wheeler AG has commissioned and successfully tested a 30 MW oxy-fired CFB pilot-scale plant in Spain [8]. Most experimental research focuses on atmospheric CFB technologies. However, CFB technology at elevated operating pressure could prove to be an additional option to use in conjunction with clean coal technology. It was reported that overall combustion efficiency increases at elevated pressure, due to higher char burn-out rate and higher heat transfer [9-11]. Furthermore, building pressurized fluidized bed systems requires less space because of their compactness [9]. Taking into account the size advantages of pressurized fluidized beds over atmospheric fluidized beds, more research on new design configurations, such as the novel design tested by Wang *et al.* [12], are still desirable for efficient utilization of certain coals. Gupta and Nag [11] have studied bed-to-wall heat transfer including hydrodynamic parameters such as voidage and suspension density in pressurized circulating fluidized beds (PCFB). Silica sand was used with particle size of 260  $\mu\text{m}$  and superficial gas velocity ranged between 0.25 m/s and 1.25 m/s. These authors have carried out experiments mostly in the bubbling fluidized bed regime rather than the fast fluidized or pneumatic transport regimes. Li *et al.* [13] also investigated minimum and terminal velocity of coal gasification materials under 2.5 MPa pressure. Results show that minimum fluidization and terminal velocity decrease with pressure. The reported fundamental studies of fluidization conducted in pressurized bubbling fluidized bed reactors are given in tab. 1.

In addition to the cold flow investigation in PCFB, some notable hot flow investigations have been found in the literature. Duan *et al.* [14] reported that higher operating pressure improves both heat transfer and carbon conversion than for atmospheric CFB reactors. MacNeil and Basu [15] investigated char combustion rate in a 5.5 kW PCFB reactor. The results show a large effect of pressure on combustion rate. Pressurized fluidized bed systems with combined cycle have been widely used in Japan, particularly for large-scale electricity generation [16]. Hong *et al.* [17] have investigated the feasibility of oxy-fuel combustion in a pressurized coal reactor by different simulation packages such as Thermoflex and Aspen plus. Their results show an increase of overall net efficiency by 3% at 1.0 MPa. Previously, a parametric study of a pressurized CFB reactor has been investigated by Kalita *et al.* [18, 19] on the same unit. The tests have covered the hydrodynamics for blended inert particles and biomass under different weight proportions. It is important to notice that these studies were conducted with relatively higher parameters, where bed pressure increased from 0.3 to 0.5 MPa while superficial gas velocities through the unit were fixed at from 5 to 7 m/sec. Granted that a few experimental studies have been conducted on the hydrodynamics of CFB at elevated operating pressure. However, studies related to the cold flow hydrodynamics of CFB under oxy-fuel conditions at elevated pressure have not been reported in detail. Previously, Komorowski and Nowak [20] have tested the effect of air and  $\text{CO}_2$  as the fluidization medium for glass beads under cold conditions. Their results showed that the axial solids distribution was non-uniform at low superficial velocity and gradually tended to uniform with increasing superficial gas velocity to 1.25 m/s. Guedea *et al.* [21] investigated the influence of  $\text{O}_2/\text{CO}_2$  mixtures on fluid dynamics in a bubbling fluidized bed (90 kW) at CIRCE, Spain. Experiments were conducted under ambient as well as high-temperature conditions. It was concluded that larger  $\text{CO}_2$  concentrations cause greater bed voidage and bed expansion. The current work studies the effect of operating pressure on hydrodynamic parameters such as bed pressure drop and voidage pro-

files. Furthermore, cold experiments were conducted with O<sub>2</sub>/CO<sub>2</sub> mixtures at atmospheric pressure to simulate oxy-fired CFB hydrodynamics.

**Table 1. Fundamental pressurized fluidized bed studies**

Authors	Bed material	$d_p$ range [mm]	Pressure [kPa]	Findings
Llop <i>et al.</i> [22]	Silica sand	0.21-1.46	1500	Prediction of bed expansion has been developed; bed expansion increases with pressure for both Geldart B and D particles.
Barreto <i>et al.</i> [23]	Silica-Alumina, zeolite	0.07-0.09	2000	Decrease of average particle size and bubble velocity observed. Bubble flow and hold up decreased with pressure; $U_{mf}$ and $U_{mb}$ increase with pressure.
Wiman and Almstedt [24]	Sand	0.45-0.70	1600	Erosion rate and average heat transfer coefficient increased with pressure.
Olowson and Almstedt [25-27]	Silica sand	0.31; 0.70; 0.98	1600	Minimum fluidization velocity decreases with pressure increases. Dense phase voidage at $U_{mf}$ does not change with pressure for small particles, while slight increase is observed for the larger particles.
Carsky and Hartman [28]	Sand	0.60	1300	Overall bubble size decreases up to 400 kPa, significant difference in bubble size for higher pressure was observed. Bubble frequency increases with excess velocity of air.
Sidorenko and Rhodes [29]	Fluid catalytic cracking, sand	0.08	101-2100	No effect of pressure was observed for particles group Geldart A, while for Geldart B particle group, $U_{mf}$ decreases slightly. Bed voidage at $U_{mf}$ found independent of operating pressure.
Richtberg <i>et al.</i> [30]	Glass beads	0.08	100-500	Homogeneous fluidization was obtained as result of bed pressure in PCFB.
Marzocchella and Salatino [31]	Glass beads	0.07-0.20	100-8000	Hydrodynamics at supercritical pressure with CO <sub>2</sub> ambient studied. Regions of homogeneous fluidization broaden due to the density of CO <sub>2</sub> fluid; fluidization was smoother under aggregative conditions.
Cao <i>et al.</i> [32]	Polystyrene beads	1.00	100-1100	Average bed voidage increases with pressure at same velocity.
Borodulya <i>et al.</i> [33, 34]	Sand	0.13-1.22	8000	Heat transfer coefficient increases from the bed to the surface.

### Experimental set-up and methodology

Hydrodynamic experiments were conducted in a small-scale CFB set-up is illustrated in fig. 1. The CFB system consists of riser, solid separator cyclone, downcomer, and auxiliaries such as air compressor and gas cylinders. The height of the CFB riser is 2000 mm with an inner diameter (ID) of 54 mm. Pressurized air was supplied by an air compressor connected to the bottom part of the riser. The height of the air plenum is 40 mm. The perforated distributor

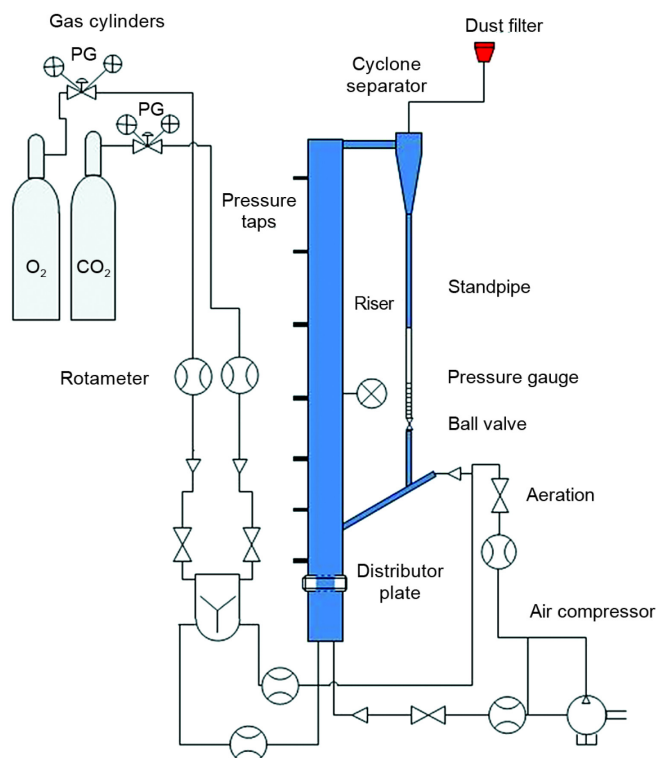


Figure 1. The CFB riser (air and O<sub>2</sub>/CO<sub>2</sub> mode)

Table 2. Calculated gas velocity [ms<sup>-1</sup>] for each mean particle size

Mean particle size [μm]	25%	50%	75%
160	1.1	1.3	1.5
302	2.1	2.5	2.9
427	2.7	3.3	3.8

determined following Kunii and Levenspiel [35]. The dimensionless values of particle size,  $d^*$ , and gas velocity,  $U^*$ , are approximated for the direct evaluation of the terminal velocity of particles. It should be noted that the gas viscosity is dependent on temperature and does not change significantly with bed pressure. With increase of gas density in the reactor due to the increasing bed pressure, the terminal velocity is expected to decrease, leading to a change of bed pressure drop. However, fixed terminal velocity values of atmospheric pressure are used for all conditions in these experiments. Experiments also included two bed inventory weights of 0.5 and 0.75 kg. The solid re-circulation rate,  $G_s$ , was measured by a transparent high-pressure plastic tube in the return leg. The accumulated solids height was measured by transparent pipe. The pressure drop along the riser was measured by a water column manometer which was fabricated with 11 reading taps. A high-pressure transparent plastic tube with ID of 10 mm was connected between pressure taps and a U-type water manometer. An extra wire mesh and cotton layer were fixed in all 11 taps to prevent escape of solid particles to the water

plate had an opening area of 17%. When an O<sub>2</sub>/CO<sub>2</sub> mixture environment was used, the O<sub>2</sub> and CO<sub>2</sub> gases were provided by cylinders as seen in fig. 1. Before feeding gases to the reactor, both CO<sub>2</sub> and O<sub>2</sub> gases were well mixed in a static cyclone mix. The static mixer has a height of 200 mm and diameter of 60 mm. Silica sand of Geldart B group was used in the experiments with three mean particle diameters of 160, 302, and 427 μm. Sauter mean diameters (SMD) of the particles ( $d_p$ ) were determined from sieve analysis as noted by Olowson and Almstedt [25]. The minimum fluidization velocity,  $U_{mf}$ , was determined from the Ergun equation. Experiments were conducted at four different operating pressures: 0.10, 0.15, 0.20, and 0.25 MPa. At each operating pressure, three superficial gas velocities were considered in terms of non-dimensional value  $U_{gas}/U_t$  as 25, 50, and 75% of terminal velocity,  $U_t$ , depending on mean particle size. Actual values of superficial gas velocity are given in tab. 2.

The terminal velocities of the mean particle sizes were de-

manometer. For uncertainty analysis, each experiment was repeated three times and average data of these experiments were taken as representative. Pressure drop,  $\Delta P_{\text{bed}}$ , profiles were photographed three times by digital camera with two seconds intervals in order to catch  $\Delta P_{\text{bed}}$  fluctuation. Higher pressure fluctuation was observed in the dense zone of the riser than in the dilute zone. This occurs due to the coarse particles which were trapped in the freeboard. Similar pressure fluctuations in the dense zone were reported by Czakiert *et al.* [36].

## Results and discussion

### Hydrodynamics at atmospheric pressure

#### Effect of superficial gas velocity on pressure drop

Superficial gas velocity ranges in this study were in the fast fluidized bed regime. Figure 2 illustrates the effect of superficial gas velocity on bed pressure drop,  $\Delta P_{\text{bed}}$ , for smaller particle size of 160  $\mu\text{m}$  at atmospheric pressure. The first two points in fig. 2 represent  $\Delta P_{\text{bed}}$  through the distributor plate. Pressure drop increases with superficial gas velocity which agrees well with the literature [37]. It is also found that the increase of superficial gas velocity affects the axial particle holdup distribution due to increasing bed expansion. From fig. 2, it can be seen that the pressure drop along the bed remains constant for lower superficial velocities, whereas for higher gas velocity the pressure drop rises slightly along the bed height, and tends to reach a constant value. The higher pressure drop observed at the bottom of the bed may be due to the fact that the particles are being accelerated by the inlet gas velocity. The effect of solids loading on the pressure drop is also plotted in the same figure at a gas velocity of 1.1 m/s. It is also noticed that the pressure drop exponentially increases with bed height when the solid loading was increased to 0.75 kg. The exponential increase of pressure drop is more pronounced at the bottom of the bed and indicates the presence of a dense solid bed. This region is called the acceleration zone. Above this region, the pressure drop increases slightly with bed height. This suggests a fully accelerated particle flow in this region. This behavior is also consistent with the literature [38].

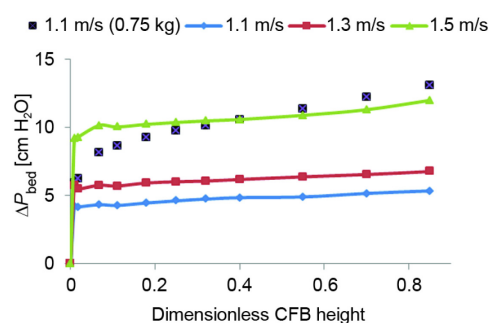


Figure 2. Effect of superficial gas velocity on  $\Delta P_{\text{bed}}$  over the bed ( $d_p = 160 \mu\text{m}$ , solids loading is 0.5 kg)

#### Effect of superficial gas velocity on bed voidage

The effect of superficial gas velocity on bed voidage is illustrated in figs. 3(a) and 3(b). The voidage in the bed was determined using pressure drop calculations. It can be noticed from fig. 3(a) that voidage profiles increase with superficial gas velocity (1.1-1.5 m/s). Increase of superficial gas velocity raises the solids holdup capacity which tends to increase voidage, which agrees with other studies [39]. It is also found from fig. 3(a) that lower voidage at the bottom of the riser is observed for all gas velocities. This may be due to the fact that the bottom region of the riser is mainly affected by particle acceleration and gas distribution. Above this region, for all gas velocities, the voidage increases exponentially, approaching

constant values near the riser exit. This exponential shape occurs when particles entering the bottom of the reactor are entrained by aeration [18]. It is clearly seen from fig. 3(a) that the developing flow region with low voidage occurs up to 0.2 m and a fully-developed region with relatively high voidage begins above 0.2 m. It is important to mention that the exponential shape of the axial profile varies with superficial gas velocity. It is also observed that the axial voidage profiles move in parallel from high voidage toward low voidage with decreasing gas velocity. The effect of particle size on the axial voidage profiles in the riser at lower gas velocities  $U_{1g} = 0.25 U_t$  of 1.1, 2.1, and 2.7 m/s, respectively, is shown in fig. 3(b). The results indicate that the increase of particle size had an obvious effect on voidage, resulting in a slight difference at the top of the riser, but significantly lower voidages at the bottom. It is also found that the voidage at the bottom of the riser is higher for the larger particle (427  $\mu\text{m}$ ) than for the smaller particle (160  $\mu\text{m}$ ). The voidage tends to distribute more at the riser bottom for the large particles in comparison to smaller particles. It has been shown that most particles are mainly found near the wall of the riser in the freeboard area [40]. Solid particles separated by the cyclone were injected into the riser with a small amount of aeration which diluted the particles near the wall. Due to the range of mean particle size distribution, the larger particles continue to remain in the dense zone at lower gas velocity, whereas the smaller particles are expected to be carried out to the top by gas velocity.

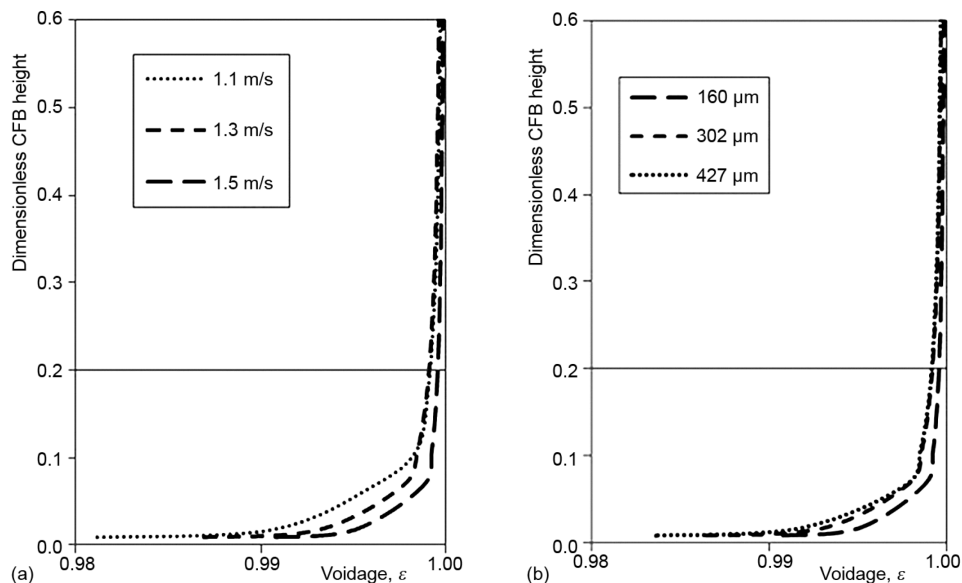


Figure 3. (a) Effect of superficial gas velocity on axial voidage profile ( $d_p = 160 \mu\text{m}$ ), (b) effect of particle size on axial voidage profile at lower gas velocity

#### *Effect of $\text{O}_2/\text{CO}_2$ mixture on bed voidage*

Industrial-scale CFB reactors operate at temperatures between 800-900 °C. The dynamic viscosity and density of gases change with operating temperature and pressure, respectively. The present case uses mixtures of  $\text{CO}_2$  and  $\text{O}_2$  gases to study the effect of density and viscosity on the cold flow hydrodynamics in the small-scale CFB riser. Only the smallest mean particle size of 160  $\mu\text{m}$  with a solids loading of 0.5 kg was tested. Figures 4(a) and 4(b) repre-

sents the voidage profiles along the height of the bed for different fluidization gases including O<sub>2</sub>/CO<sub>2</sub> mixtures and air at superficial gas velocities 1.1 and 1.5 m/s ( $U_{1g}$  and  $U_{3g}$ ). It is important to mention that the dynamic viscosity of gases does not change with pressure, while the density can be evaluated following by Li *et al.* [13]. Comparing O<sub>2</sub>/CO<sub>2</sub> mixtures with air, the axial voidage profile shows a difference in both the dense and freeboard zones of the riser for the lower superficial gas velocity; *i. e.*, in the case of air, the axial profile of voidage is higher than that in O<sub>2</sub>/CO<sub>2</sub>. This behavior may be due to the higher density of the O<sub>2</sub>/CO<sub>2</sub> mixture compared to air. When superficial gas velocity increased to 1.5 m/s ( $U_{3g}$ ), no difference in axial voidage was observed between O<sub>2</sub>/CO<sub>2</sub> mixtures and air. Identical results were reported by Komorowski and Nowak [20]. These authors observed that a low superficial gas velocity of O<sub>2</sub>/CO<sub>2</sub> mixture produced a large difference in suspension density profile compared to air, while at higher velocity, the profiles were similar. It can be concluded that in the fast fluidization regime, the axial voidage profile of O<sub>2</sub>/CO<sub>2</sub> mixture is similar to that for an air-fluidized CFB. In addition, similar heat transfer rates could be expected from identical voidage or suspension density profiles in air and O<sub>2</sub>/CO<sub>2</sub> mixture gases. However, it should be noted that, for highly exothermic reactions such as occur in coal-fired CFB combustors, good temperature control can be achieved because of the intensive mixing and circulation rate. It is also important to highlight that CO<sub>2</sub> has higher heating capacity compared to nitrogen. For this reason, the combustion temperature in oxy-fired furnaces is moderated by flue gas recirculation [41].

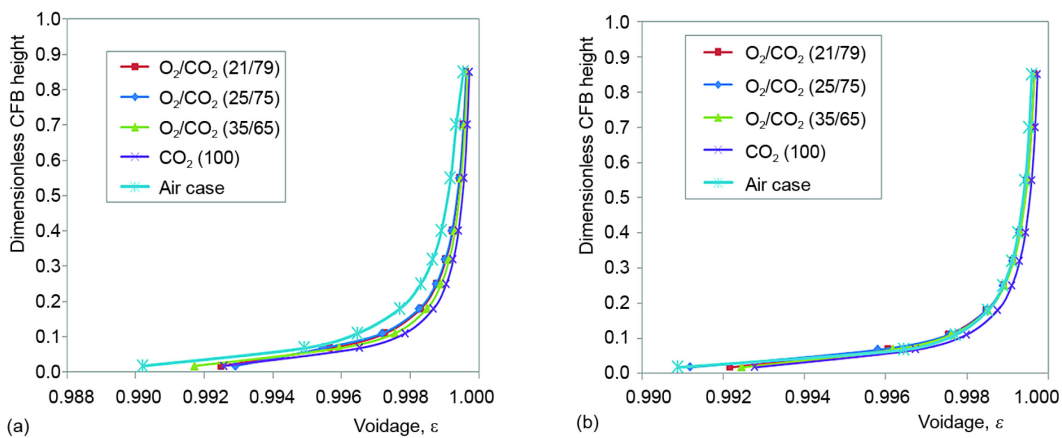


Figure 4. (a) Bed voidage vs. O<sub>2</sub>/CO<sub>2</sub> mixture (gas velocity is 1.1 m/s, solids loading is 0.5 kg), (b) bed voidage vs. O<sub>2</sub>/CO<sub>2</sub> mixture (gas velocity is 1.5 m/s, solids loading is 0.5 kg)

### Effect of operating pressure on hydrodynamic properties

#### Effect of operating pressure on pressure drop

Pressure drop ( $\Delta P_{bed}$ ) along the height of the riser was measured at different operating pressures from 0.10 to 0.25 MPa. Figure 5 illustrates pressure drop profiles along the bed riser at the lower superficial gas velocity of 2.1 m/s ( $U_{1g}$ ) for the particle size of 302  $\mu$ m. It can be seen from the fig. 5 that operating bed pressure has a clear effect on the bed pressure drop. The total pressure drop,  $\Delta P_{bed}$  from 0.10 MPa (atmospheric pressure) to 0.25 MPa, increases from 10 cm H<sub>2</sub>O to 15 cm H<sub>2</sub>O, respectively. Small fluctuations were observed at 0.20 and 0.25 MPa in the acceleration zone due to the aeration of gas, while at the fully developed zone

it increases exponentially over the bed height. As discussed by Yin *et al.* [42] the operating pressure conditions in the bed could lead to the decrease of superficial gas velocity in the reactor. This consequently results in a decrease of particle velocity. This means that more solid particles were found in the riser, leading to the higher pressure drop in the bed. Additionally, the effect of solids loading (0.75 kg) is also illustrated in fig. 5 at the operating pressure of 0.25 MPa, which shows higher pressure drop compared to the same case with bed inventory of 0.5 kg. This is due to the accumulation of additional bed material mass in the bed which leads to the further increase of bed pressure drop. Also it is found that the pressure drop gradually increases with the riser bed height. Similar observations were found by Richtberg *et al.* [30]. They observed an exponentially increasing trend at higher pressure (0.50 MPa) for bed pressure drop with glass beads. Figure 6 shows the effect of particle size of 160, 302, and 427  $\mu\text{m}$  on pressure drop ( $\Delta P_{\text{bed}}$ ) for the operating pressure of 0.20 MPa, at the gas superficial velocity ( $U_{2g} = 0.50 U_t$ ) of 1.3, 2.5, and 3.3 m/s, respectively. It can be noted from fig. 6 that the increase of particle size leads to increasing bed pressure drop. This could be due to the fact that smaller particles have less drag force compared to the larger particles. Also, it is found that for all particle sizes, the pressure drop increases exponentially with riser height. The effect of gas superficial velocity on pressure drop ( $\Delta P_{\text{bed}}$ ) at elevated pressure (0.20 MPa) for a particle size of 160  $\mu\text{m}$  is shown in fig 7. It is found that the bed pressure increases with gas superficial velocity. This may be due to the fact that an increase in gas superficial velocity results in an increase of drag force on the particles, which leads to increasing solid particle distribution in the bed. As a result, higher bed pressure is generated for higher gas velocity at fixed operating pressure. It can also be seen from the fig. 7 that the higher superficial gas velocity results in high fluctuations of pressure drop in the dense zone of the bed.

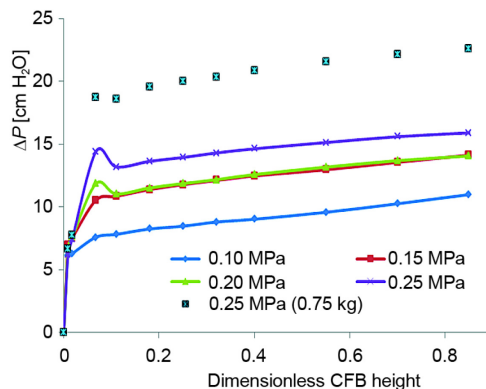


**Figure 5.** Effect of operating pressure on pressure drop at gas velocity 2.1 m/s ( $d_p = 302 \mu\text{m}$ , solids loading is 0.5 kg)

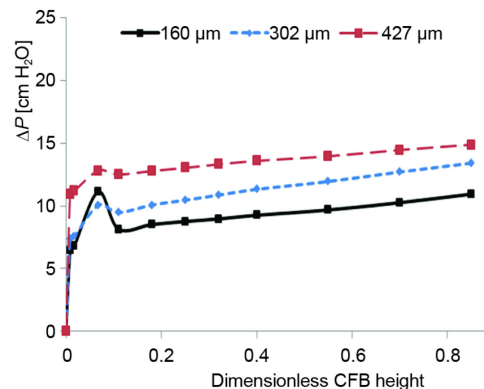


**Figure 6.** Effect of mean particle size on pressure drop at superficial gas velocity of 50% of  $U_t$  and bed pressure is 0.20 MPa

#### *Effect of operating pressure on axial bed voidage*

The voidage profiles of the riser are illustrated in fig. 8 for the superficial gas velocity of 2.1 m/s ( $U_{1g}$ ) at different bed operating pressures (0.10 to 0.25 MPa). This plot is shown for the particle size of 302  $\mu\text{m}$ . It can be seen that operating pressure in the bed decreases the voidage along the riser, particularly in the acceleration zone (dense zone). This could be

due to the increase of bed pressure. The pressurized state of the bed leads to the decrease of gas velocity which results in particle accumulation in the bottom zone of the bed. Similar observations were made by Yin *et al.* [42]. Also it can be seen that the exponential shape of the axial profile varies for different operating pressures and the developing flow region; *i. e.*, the change from high to low voidage occurs mainly up to 0.5 m. The effect of higher solids loading (0.75 kg) is also included in fig. 8 to demonstrate its effect on the voidage profile in the riser. It can be seen from fig. 8 that at the bottom of the riser, the voidage profiles show a similar trend, whereas higher voidage is observed above the dense zone of the riser for higher solid loading. The influence of mean particle size

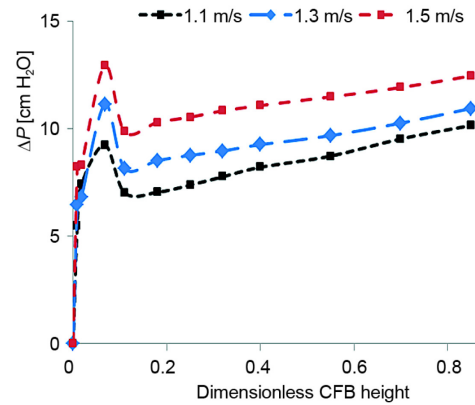


**Figure 7. Effect of superficial gas velocity on pressure drop at operating pressure of 0.20 MPa**

on the axial voidage profile at superficial gas velocity of 50% ( $U_t$ ) is illustrated in fig. 9. As expected, the larger particle size develops higher voidage at the bottom dense zone of the riser than does the smaller particle. It is also found that the voidage tends to distribute more at the riser bottom for large particles while for smaller particles, voidage is more or less uniform. The effect of superficial gas velocity on axial voidage is plotted in fig. 10, at the higher operating pressure of 0.25 MPa for particle size of 160  $\mu\text{m}$ . It is found that the axial voidage profiles increase with increasing superficial gas velocity, similar to the atmospheric pressure case. This is due to the fact that the increase of superficial gas velocity causes the solids to distribute in the riser, which tends to increase the voidage in the bed. It is also found from the fig. 10 that low voidages near the bottom of the riser are observed for higher gas velocity due to particle acceleration and gas distribution. Above this region, for all gas velocities, the voidage increases exponentially, eventually approaching a constant value near the riser exit. It is important to mention from the fig. 10 that the developing flow region occurs up to about 0.35 m and a fully-developed region with relatively high voidage begins above 0.35 m height.

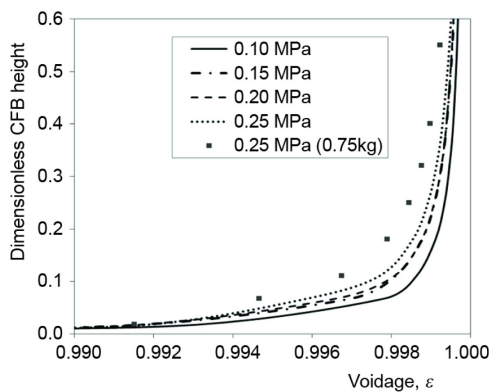


**Figure 8. Voidage profile along the height for the fixed particle size ( $d_p = 302 \mu\text{m}$ , gas velocity is 2.1 m/s, solids loading is 0.5 kg)**

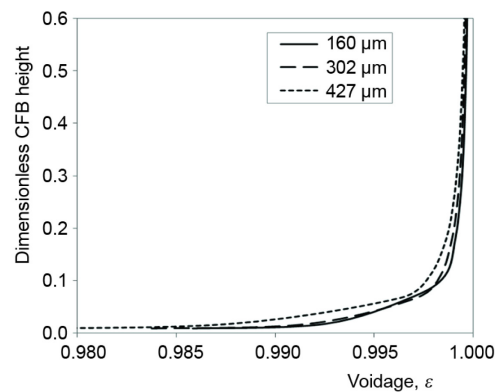


**Figure 9. Effect of mean particle size on axial voidage (gas velocity 50% of  $U_t$ , bed pressure is 0.20 MPa, solids loading is 0.5 kg)**

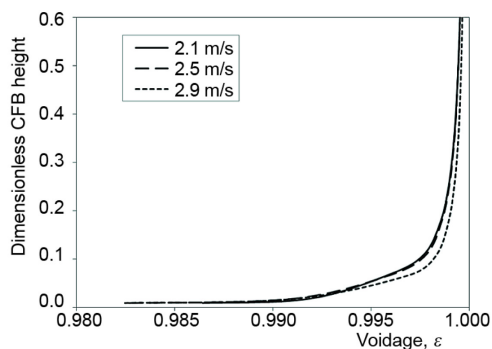


**Figure 10.** Axial voidage profile along the riser height at operating pressure 0.25 MPa ( $d_p = 302 \mu\text{m}$ , superficial gas velocities are 2.1, 2.5, and 2.9 m/s)

These values are different from those found in the atmospheric pressure case.

Overall, it can be concluded that operating pressure has a significant effect on hydrodynamic parameters in the cold flow environment. It should be mentioned that even at low operating pressure as mentioned in this work (0.25 MPa), the pressure drop increased from 10 to 15 (cm H<sub>2</sub>O) and 22 (cm H<sub>2</sub>O in) at increased solids loaded case. According to previous studies of hydrodynamics as presented in tab. 2, more pronounced effect of hydrodynamic parameters could be expected with increase of operating bed pressure. In the case of cold flow hydrodynamics of O<sub>2</sub>/CO<sub>2</sub> mixtures, it should be noted that at fast fluidized bed and pneumatic transport regimes, no significant differences are noted between O<sub>2</sub>/CO<sub>2</sub> mixtures and air. Increasing interest in pressurized CFB over atmospheric CFB and change in size configuration should always lead to a detailed hydrodynamic investigation, particularly in cold flow environment.

These observations agree with previously reported studies. In the case of O<sub>2</sub>/CO<sub>2</sub> mixtures, a notable effect of different O<sub>2</sub>/CO<sub>2</sub> proportions on axial voidage was seen at the dense zone of the riser, compared to the voidage measured when air was used. However, with further increase of superficial gas velocity from 1.1 to 1.5 m/s, these differences in axial voidage disappeared. The overall pressure drop profile increases with operating bed pressure, which agrees well with the literature. Increased solids loading appear to increase hydrodynamic parameters. Also, increase of particle size and superficial gas velocity at elevated pressure resulted to increase of bed pressure drop and axial voidage profiles, respectively.

### Acknowledgment

The authors would like to acknowledge Project FP7 iComfluid (International collaboration on computational modelling of fluidized bed systems for clean energy technologies), No. 212261 for funding this work in the context of development of clean coal technologies in India.

### Nomenclature

$d_p$  – particle diameter, [ $\mu\text{m}$ ]  
 $G_s$  – solids recirculation rate, [ $\text{kgm}^{-2}\text{s}^{-2}$ ]  
 $U_{\text{gas}}$  – superficial gas velocity, [ $\text{ms}^{-1}$ ]  
 $U_{\text{mb}}$  – bubble velocity, [ $\text{ms}^{-1}$ ]  
 $U_{\text{mf}}$  – minimum fluidization velocity, [ $\text{ms}^{-1}$ ]  
 $U_t$  – terminal velocity, [ $\text{ms}^{-1}$ ]  
 $\Delta P_{\text{bed}}$  – bed pressure drop, [ $\text{cmH}_2\text{O}$ ]

### Acronyms

ID – inner diameter  
 CFB – circulating fluidized bed  
 PCFB – pressurized CFB  
 PG – pressure gauge

### Conclusions

A hydrodynamic cold flow study of silica sand was undertaken with air and O<sub>2</sub>/CO<sub>2</sub> mixtures as the fluidization medium at atmospheric pressure. Additionally, experiments were conducted with air at elevated operating pressure to investigate the pressure effect on hydrodynamic parameters. The increase of bed pressure drop ( $\Delta P_{\text{bed}}$ ) along the bed height is similar for all three superficial gas velocities. The effect of superficial gas velocity and particle size on axial bed voidage profiles shows an increasing trend as expected.

## References

- [1] \*\*\*, IEA, Key World Energy Statistics, International Energy Agency, 2012
- [2] Basu, P., Combustion of Coal in Circulating Fluidized-Bed Boilers: A Review, *Chem. Eng. Sci.*, 54 (1999), 22, pp. 5547-5557
- [3] Beer, J. M., High Efficiency Electric Power Generation: The Environmental Role, *Prog. Energy Combust. Sci.*, 33 (2007), 2, pp. 107-134
- [4] Grace, J. R., et al., *Circulating Fluidized Beds*, Blackie Academic & Professional, London, 1997
- [5] Nowak, W., Clean Coal Fluidized-Bed Technology in Poland, *Appl. Energy.*, 74 (2003), 3-4, pp. 405-413
- [6] Anthony, E. J., Oxyfuel CFBC: Status and Anticipated Development, *Greenh. Gases Sci. Technol.*, 3 (2013), 2, pp. 116-123
- [7] Tan, Y., et al., Experiences and Results on a 0.8 MWth Oxy-Fuel Operation Pilot-Scale Circulating Fluidized Bed, *Appl. Energy.*, 92 (2012), Apr., pp. 343-347
- [8] Lupion, M., et al., 30 MWth CIUDEN Oxy-CFB Boiler – First Experiences, *Energy Procedia*, 37 (2013), Dec., pp. 6179-6188
- [9] Niksa, S., et al., Coal Conversion Submodels for Design Applications at Elevated Pressures, Part I, Devolatilization and Char Oxidation, *Prog. Energy Combust. Sci.*, 29 (2003), 5, pp. 425-477
- [10] Huang, Y., et al., Influences of Coal Type on the Performance of a Pressurized Fluidized Bed Combustion Power Plant, *Fuel*, 79 (2000), 13, pp. 1595-1601
- [11] Gupta, A. V. S. S. K. S., Nag, P. K., Bed-to-Wall Heat Transfer Behavior in a Pressurized Circulating Fluidized Bed, *Int. J. Heat Mass Transf.*, 45 (2002), 16, pp. 3429-3436
- [12] Wang, A. T. L., et al., Hydrodynamic Performance of a Novel Design on Pressurized Fluidized Bed Combustor, *J. Energy Resour. Technol.*, 128 (2006), 2, pp. 111-117
- [13] Li, J., et al., Minimum and Terminal Velocity in Fluidization of Coal Gasification Materials and Coal Blending of Gasification Under Pressure, *Fuel*, 110 (2013), Aug., pp. 153-161
- [14] Duan, F., et al., Dependence of Bituminous Coal Gasification on Pressure in a Turbulent Circulating Fluidized Bed, *Asia-Pacific J. Chem. Eng.*, 7 (2012), 6, pp. 822-827
- [15] MacNeil, S., Basu, P., Effect of Pressure on Char Combustion in a Pressurized Circulating Fluidized Bed Boiler, *Fuel*, 77 (1998), 4, pp. 269-275
- [16] Stubington, J. F., Wang, A. L. T., Unburnt Carbon Elutriation from Pressurized Fluidized Combustion of Australian Black Coals, *Fuel*, 79 (2000), 10, pp. 1155-1160
- [17] Hong, J., et al., Analysis of Oxy-Fuel Combustion Power Cycle Utilizing a Pressurized Coal Combustor, *Energy*, 34 (2009), 9, pp. 1332-1340
- [18] Kalita, P., et al., Parametric Study on the Hydrodynamics and Heat Transfer Along the Riser of a Pressurized Circulating Fluidized Bed Unit, *Exp. Therm. Fluid Sci.*, 44 (2013), Jan., pp. 620-630
- [19] Kalita, P., et al., Effect of Biomass Blending on Hydrodynamics and Heat Transfer Behavior in a Pressurized Circulating Fluidized Bed Unit, *Int. J. Heat Mass Transf.*, 60 (2013), May, pp. 531-541
- [20] Komorowski, M., Nowak, W., Vertical Solids Distribution under Air/Carbon Dioxide Fluidization Conditions in a Circulating Fluidized Bed, *Proceedings*, 14<sup>th</sup> International Conference on Fluidization – From Fundamentals to Products, Noordwijkerhout, The Netherlands, 2013
- [21] Guedea, I., et al., Influence of O<sub>2</sub>/CO<sub>2</sub> Mixtures on the Fluid-Dynamics of an Oxy-Fired Fluidized Bed Reactor, *Chem. Eng. J.*, 178 (2011), Dec., pp. 129-137
- [22] Llop, M. F., et al., Expansion of Gas-Solid Fluidized Beds at Pressure and High Temperature, *Powder Technol.*, 107 (2000), 3, pp. 212-225
- [23] Barreto, G. F., et al., The Effect of Pressure on the Flow of Gas in Fluidized Beds of Fine Particles, *Chem. Eng. Sci.*, 38 (1983), 12, pp. 1935-1945
- [24] Wiman, J., Almstedt, A. E., Hydrodynamics, Erosion and Heat Transfer in a Pressurized Fluidized: Influence of Pressure, Fluidization Velocity, Particle Size and Tube Bank Geometry, *Chem. Eng. Sci.*, 52 (1997), 16, pp. 2677-2695
- [25] Olowson, P. A., Almstedt, A. E., Influence of Pressure on the Minimum Fluidization Velocity, *Chem. Eng. Sci.*, 46 (1991), 2, pp. 637-640
- [26] Olowson, P. A., Influence of Pressure and Fluidization Velocity on the Hydrodynamics of a Fluidized Bed Containing Horizontal Tubes, *Chem. Eng. Sci.*, 49 (1994), 15, pp. 2437-2446
- [27] Olowson, P. A., Almstedt, A. E., Hydrodynamics of a Bubbling Fluidized Bed: Influence of Pressure and Fluidization Velocity in Terms of Drag Force, *Chem. Eng. Sci.*, 47 (1992), 2, pp. 357-366

- [28] Carsky, M., Hartman, M., The Bubble Frequency in a Fluidized Bed at Elevated Pressure, *Powder Technol.*, 61 (1990), 3, pp. 251-254
- [29] Sidorenko, I., Rhodes, M. J., Influence of Pressure on Fluidization Properties, *Powder Technol.*, 141 (2004), 1, pp. 137-154
- [30] Richtberg, M., et al., Characterization of the Flow Patterns in a Pressurized Circulating Fluidized Bed, *Powder Technol.*, 155 (2005), 2, pp. 145-152
- [31] Marzocchella, A., Salatino, P., Fluidization of Solids with CO<sub>2</sub> at Pressures from Ambient to Supercritical, *AIChE J.*, 46 (2000), 5, pp. 901-910
- [32] Cao, J., et al., Simulation and Experimental Studies on Fluidization Properties in a Pressurized Jetting Fluidized Bed, *Powder Technol.*, 183 (2008), 1, pp. 127-132
- [33] Borodulya, V. A., Heat Transfer between a Surface and a Fluidized Bed: Consideration of Pressure and Temperature Effects, *Int. J. Heat Mass Transf.*, 34 (1991), 1, pp. 47-53
- [34] Borodulya, V. A., et al., Heat Transfer between Fluidized Bed of Large Particles and Horizontal Tube Bundles at High Pressures, *Int. J. Heat Mass Transf.*, 27 (1984), 8, pp. 1219-1225
- [35] Kunii, D., Levenspiel, O., *Fluidization Engineering*, 2<sup>nd</sup> ed, Butterworth Heinemann., London, 1991
- [36] Czakiert, T., et al., Oxy-Fuel Circulating Fluidized Bed Combustion in a Small Pilot-Scale Test Rig, *Fuel Process. Technol.*, 91 (2010), 11, pp. 1617-1623
- [37] Sanchez-Delgado, S., et al., On the Minimum Fluidization Velocity in 2D Fluidized Beds, *Powder Technol.*, 207 (2011), 1, pp. 145-153
- [38] Chew, J. W., et al., Reverse Core-Annular Flow of Geldart Group B Particles in Risers, *Powder Technol.*, 221 (2012), May, pp. 1-12
- [39] Das, M., et al., Axial Voidage Profiles and Identification of Flow Regimes in the Riser of a Circulating Fluidized Bed, *Chem. Eng. J.*, 145 (2008), 2, pp. 249-258
- [40] Mahmoudi, S., et al., Solids Flow Diagram of a CFB Riser Using Geldart B-Type Powders, *Particology*, 10 (2012), 1, pp. 51-61
- [41] Buhre, B. J. P., et al., Oxy-Fuel Combustion Technology for Coal-Fired Power Generation, *Prog. Energy Combust. Sci.*, 31 (2005), 4, pp. 283-307
- [42] Yin, S., et al., Gas-Solid Flow Behavior in a Pressurized High-Flux Circulating Fluidized Bed Riser, *Chem. Eng. Commun.*, 201 (2014), 1, pp. 352-366